ChemSICal: Evaluating a Stochastic Chemical Reaction Network for Molecular Multiple Access

Alexander Wietfeld, Marina Wendrich, Sebastian Schmidt, Wolfgang Kellerer
Chair of Communication Networks
Technical University of Munich, Germany
{alexander.wietfeld, marina.wendrich, sebastian.a.schmidt, wolfgang.kellerer}@tum.de

***Abstract*—Proposals for molecular communication networks as part of a future internet of bio-nano-things have become more intricate and the question of practical implementation is gaining more importance. One option is to apply detailed chemical modeling to capture more realistic effects of computing processes in biological systems. In this paper, we present ChemSICal, a detailed model for implementing the successive interference cancellation (SIC) algorithm for molecular multiple access in diffusion-based molecular communication networks as a chemical reaction network (CRN). We describe the structure of the model as a number of smaller reaction blocks, their speed controlled by reaction rate constants (RRCs). Deterministic and stochastic methods are utilized to first iteratively improve the choice of RRCs and subsequently investigate the performance of the model in terms of an error probability. We analyze the model's sensitivity to parameter changes and find that the analytically optimal values for the non-chemical model do not necessarily translate to the chemical domain. This necessitates careful optimization, especially of the RRCs, which are crucial for the successful operation of the ChemSICal system.**

***Index Terms*—molecular communication, chemical reaction networks, NOMA, successive interference cancellation**

I. Introduction

Diffusion-based molecular communication (DBMC) is a communication paradigm that utilizes molecules as information carriers. As a biocompatible, energy-efficient and natively nano-scale solution, DBMC could facilitate information exchange in a future internet of bio-nano-things (IoBNT), where biological environments like the human body are accessible to networking. The realization of the IoBNT could enable revolutionary medical use case such as targeted drug delivery or advanced monitoring and diagnosis [1], [2]. Nodes within these DBMC networks are expected to be natural or synthetic structures on the micro- and nanoscale. The field of bioengineering has seen significant progress in recent years and engineered cells or bacteria can function as devices with specific but limited capabilities [1]. To realize the envisioned complex applications, the establishment of DBMC networks for communication and cooperation is necessary.

A. State of the Art

As one of the first steps towards more communication participants, multiple access (MA) has been an important topic of investigation for DBMC research. Proposals include time-division multiple access (TDMA) [3], where transmitters (TXs) are assigned individual time slots and have to wait for their turn to transmit, or molecule-division multiple access (MDMA) [4], where each TX uses a different molecule type to communicate and the receiver (RX) can, therefore, differentiate them chemically. To combine the simultaneous transmissions from MDMA and the use of only a single molecule type from TDMA, non-orthogonal multiple access (NOMA) has been proposed as a possible solution [5]. To realize NOMA, the implementation of successive interference cancellation (SIC) at the RX is necessary to differentiate the TXs based on the number of received molecules. NOMA for DBMC networks (DBMC-NOMA) has been investigated from an analytical point of view [5]. However, the implications of implementing such an algorithm in a biological environment within tiny low-capability devices has not been addressed. In contrast to classical communication systems, DBMC networks will not have access to general-purpose computing resources. As a result, the notion of chemical reaction networks (CRNs) has gained significant research attention. Vasić et al. discuss the capabilities of CRNs and describe several examples, which are capable of executing simple functionalities like comparison or addition [6]. An example of a simple CRN can be seen in Figure 1. Each reaction is described by reactants or input species, products or output species, and a reaction rate constant (RRC) that determines the speed with which the reaction occurs. In this case, the species A and B form the inputs, and their concentrations, denoted as $\mathbb{N}(A), \mathbb{N}(B)$ together form the concentration of the output species C, as $\mathbb{N}(C) = \mathbb{N}(A) + \mathbb{N}(B)$, after the system has reached a steady-state, thereby implementing addition. Other researchers have specifically targeted DBMC networks. For example, Bi et al. investigated and implemented several simple functionalities such as logic gates and amplification in the form of CRNs for use in a molecular communication node. Since chemical reactions are governed by stochastic processes, deterministic models do not capture their behavior fully, and it is important to also utilize stochastic chemical reaction network (SCRN) models [7]. In [7], Heinlein et al. model a RX with multiple

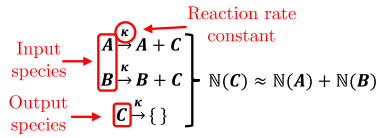

Fig. 1. Example of a simple chemical reaction network computing the sum of two inputs A and B as a third chemical species C.

The authors acknowledge the financial support by the Federal Ministry of Education and Research of Germany in the program of "Souverän. Digital. Vernetzt.". Joint project 6G-life, project identification number: 16KISK002.

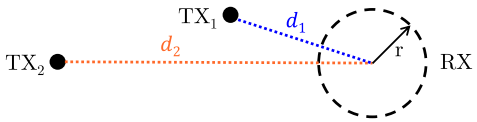

Fig. 2. Simple DBMC network with 2 point TXs and a passive spherical RX

functionalities such as detection and synchronization solely using SCRNs. Angerbauer et al. have used chemical reactions to model simple neural network architectures that could be used in future DBMC communication nodes [8]. However, CRNs have not previously been used in the context of DBMC networks to implement multi-node capabilities such as MA, which will be crucial in the IoBNT.

B. Contributions

In this work, we present the following contributions.

- We propose ChemSICal, a model for chemical implementation of SIC for MA in a simple DBMC network, expanding our initial proposal in [9].
- We use deterministic and stochastic methods to optimize the network and evaluate the impact ChemSICal has on the algorithm performance.
- We conduct a sensitivity analysis of selected parameters to show that the RRCs values are critical for the system's performance and that analytically optimal parameters might not be optimal in the chemical model. It will be necessary to adapt the algorithm to the chemical implementation, even at the cost of deviating from the analytically optimal parameters.

II. System Model

In the following, a communication scenario is presented forming the underlying framework in which the ChemSICal model will be tested. Additionally, the concepts of DBMC-NOMA and the SIC algorithm will be explained.

A. Communication Scenario

To put the proposed SIC model in context, we look at a simplified communication scenario, in which we can employ ChemSICal on the RX side. In the following, we will describe the underlying assumptions regarding the network and communication system. In Figure 2, a DBMC network is depicted with 2 TXs at distances $d_1 \leq d_2$ from a single RX. The RX is modeled as a passive spherical observer of the molecules within its receiving volume $V_{\mathrm{RX}} = \frac{4}{3}\pi r^3$, where r is the RX radius. The TXs are assumed to be 1D points capable of instantaneously emitting pulses of N_{TX} molecules. Given a free diffusion channel with diffusion coefficient D, the average received number of molecules over time at the RX, $\lambda_i(t)$, following a pulse from TX_i at time $t = 0$ is [10]

$$\lambda_i(t) = \frac{N_{\mathrm{TX}} V_{\mathrm{RX}}}{(4\pi D t)^{\frac{3}{2}}} \exp\left(-\frac{d_i^2}{4Dt}\right) \quad \text{for } t \geq 0. \tag{1}$$

Furthermore, we assume that the TXs use on-off-keying (OOK) to transmit binary information symbols $s_i \in \{0, 1\}$ by emitting none or N_{TX} molecules, respectively. The system is fully synchronized and for the sake of simplicity, we neglect the inter-symbol interference (ISI) on the basis that the symbol period between subsequent pulses must be sufficiently large. As a result, we will focus on a single symbol period, in which the RX takes a single sample n_{s} at the peak time t_{p} of the received number of molecules. In this work, the DBMC-NOMA scheme with SIC, as defined in [5] and described in Section II-B, is implemented. Therefore, both TXs transmit at the same time, denoted as $t = 0$, using the same molecule type. As diffusion is a stochastic process, the instantaneous received number of molecules is commonly modeled as a Poisson-distributed random variable [11]. The RX will observe the sum of the two independent Poisson variables corresponding to the received signal from each TX. The sum of two independent Poisson variables is a Poisson variable and the sample at the RX is therefore, $n_{\mathrm{s}} \sim \mathcal{P}\left(s_1\lambda_1(t_p) + s_2\lambda_2(t_p)\right)$. The probability distribution of n_{s} can be further specified, given that the four different symbol combinations in $\{[s_1 s_2], s_1, s_2 \in \{0, 1\}\}$ are assumed to be equiprobable. Then, the probability mass function (PMF) for the sample at the RX is given by

$$p_{n_{\mathrm{s}}}[n] = \frac{1}{4} \cdot \left(\mathcal{P}_{\mathrm{PMF}}(n; 0) + \mathcal{P}_{\mathrm{PMF}}(n; \lambda_2) + \mathcal{P}_{\mathrm{PMF}}(n; \lambda_1) + \mathcal{P}_{\mathrm{PMF}}(n; \lambda_1 + \lambda_2)\right), \tag{2}$$

where $\mathcal{P}_{\mathrm{PMF}}(n; \lambda) = \lambda^n \frac{e^{-\lambda}}{n!}$ is the PMF of the Poisson distribution at n.

B. NOMA and Successive Interference Cancellation

The theoretical basis for symbol differentiation at the RX is the SIC algorithm as presented in [12]. An adaptive threshold detection system is employed resulting in a binary tree decision structure depicted in Figure 3. It is based on the assumption that the received numbers of molecules from the TXs differ in magnitude. This can be facilitated through different mechanisms. One option is to optimize the numbers of emitted molecules, for example, using a pilot-symbol-based algorithm [12]. In order to focus primarily on the CRN implementation, consideration of the optimization algorithm in the chemical domain is left for future work. In this investigation we will assume that due to the random diffusive nature of DBMC systems, it is very unlikely for two TXs to be at the same distance from the RX at a particular time. Therefore, the average received numbers of molecules obey the relation $\lambda_1 > \lambda_2$, due to the assumption that $d_1 > d_2$ [13]. The SIC algorithm then works as follows. The acquired sample n_{s} is compared in multiple steps. In the first step, the symbol for TX_1, $\hat{s}_1$, is detected and in the second step, the threshold depends on the first step, yielding the symbol $\hat{s}_2$ for TX_2, as shown in the following:

$$\hat{s}_1 = \begin{cases} 1 & n_{\mathrm{s}} \geq \tau_1 \\ 0 & \text{otherwise.} \end{cases} \tag{3} \qquad \hat{s}_2 = \begin{cases} 1 & n_{\mathrm{s}} \geq \tau_1^{\hat{s}_1} \\ 0 & \text{otherwise.} \end{cases} \tag{4}$$

This structure is theoretically extendable to arbitrary numbers of TXs [12] but we focus on the case of 2 TXs for this work.

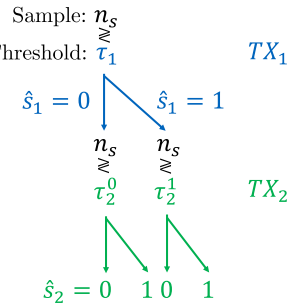

Fig. 3. Simplified SIC algorithm for DBMC [12]. Example for 2 TXs.

III. ChemSICal Design

The analysis of a network using DBMC-NOMA has been conducted in [5], [13], yielding optimal values for the detection thresholds given a certain distance constellation, but without considering the chemical implementation of the SIC algorithm. Therefore, our aim is to frame the algorithm as a chemical computing problem and to propose ChemSICal, a chemical reaction network for SIC. As detailed in Section I, a CRN is a set of coupled chemical reactions consisting of different species of molecules, reactant-product relations, and RRCs. Firstly, we will define the desired input and output species. To create a link between the underlying DBMC-NOMA system and the CRN on the RX side, the signaling molecule type is defined to be of the input species Y_{on}. Consequently, the number of molecules n_{s} sampled by the RX as detailed in Section II-A is used as the initial concentration of the Y_{on} molecules for the CRN. We denote the species by its name, e.g., Y_{on}, and the corresponding number of molecules with $\mathbb{N}(Y_{\text{on}})$. After a number of chemical reactions occur, as will be described in the next section, we end up with output species D_i^0, D_i^1 with $i \in \{1, 2\}$ for both TXs. The symbols detected by the CRN, $\hat{s}_i^C$, are determined via the number of output species molecules as follows:

$$\hat{s}_i^C = \begin{cases} 1 & \mathbb{N}(D_i^1) \geq \mathbb{N}(D_i^0) \\ 0 & \mathbb{N}(D_i^0) > \mathbb{N}(D_i^1). \end{cases} \tag{5}$$

A. CRN Block Diagram

Figure 4 depicts the logical structure of ChemSICal. In order to keep the overview of the proposal as simple as possible, as well as collect related reactions in logically coherent units, we utilize reaction blocks, capable of executing simpler operations such as comparisons or additions, each consisting of up to four individual chemical reactions. To implement ChemSICal, we need the following reaction blocks, as described in [6]:

- *Comparison:* Compares an input species (Y_{on}) to a threshold (W_i) and generates two indicator molecule species ($X_{\text{on},i}$, $X_{\text{off},i}$), the ratio of which indicates the ratio between input and threshold.
- *Translation:* From one or multiple inputs ($X_{\text{on},i}$, $X_{\text{off},i}$), generates detection molecule species (D_i^0, D_i^1) of the exact same number. This is used to decouple subsequent reactions, i.e., limit interference of the previous reaction on the reactants of the following ones.
- *Approximate Majority:* Takes two inputs (D_i^0, D_i^1) and greatly amplifies any differences in numbers between them, i.e., turns $\mathbb{N}(D_i^j) > \mathbb{N}(D_i^k)$ into outputs $\mathbb{N}(D_i^j) \gg \mathbb{N}(D_i^k)$. This results in an approximate binary decision, where many more of one species, and almost none of the other are left.
- *Threshold Adaptation:* Essentially corresponds to an addition CRN, as shown in Figure 1, where the base threshold species, $W_{2,\text{B}}$, and the resulting detection species D_1^1 are added to form the threshold species W_2. This links the first stage for detecting the bit from TX_1 with the second stage for the bit from TX_2. The numbers from each species must be tuned such that the following holds: $\mathbb{N}(W_{2,\text{B}}) = \tau_2^0$ and $\mathbb{N}(X_{\text{on},1}) + \mathbb{N}(X_{\text{off},1}) + \mathbb{N}(W_{2,\text{B}}) = \tau_2^1$. The latter must hold, since $\mathbb{N}(D_1^1) \approx \mathbb{N}(X_{\text{on},1}) + \mathbb{N}(X_{\text{off},1})$ after the first-stage *Approximate Majority* block in case of $\hat{s}_1^C = 1$.

Each reaction block is associated with a particular RRC, as denoted under the blocks in Figure 4. Every reaction in each block uses this RRC. The exact reactions with intermediary molecule species can be found in [9], and are adapted from [6]. Importantly, the sequential nature implied by the arrows in Figure 4 is purely logical and to make the diagram more easily understandable. In fact, the reaction are all started at the same time and run in parallel to each other. Therefore, no additional external control over the CRN is required.

B. Solvers and Evaluation Metrics

In the following, we will define the metrics used for the subsequent evaluation of the ChemSICal model. They are based on the detection outcome $\hat{s}_i^C$, as defined above. The correctness of the result depends on the input value Y_{on}, i.e. the underlying received signal n_{s}, which dictates the expected outcome according to the non-chemical SIC algorithm in Figure 3. Additionally, the appropriate metric depends on the type of solver that is applied to the CRN. We will use both a deterministic and a stochastic solver for the evaluation. The deterministic solver converts the entire CRN into a set of ordinary differential equations (ODEs) and finds the solution as a continuous time-varying function of each species' concentration [14]. The deterministic approaches cannot capture the probabilistic dynamics of CRNs, especially in cases where the molecule concentration is low [14]. Therefore, we also apply a stochastic simulation algorithm (SSA) solver, which uses a time-continuous value-discrete Markov process and the well-known Gillespie's algorithm [15]. The latter generates a statistically accurate sample trajectory of the system [14]. Subsequently, a Monte Carlo simulation using N_{traj} trajectories is conducted to gain more insight into the statistical properties of the system. The following metrics will be used:

1) *Correct Detection*: We define the binary indicator for a correct outcome given a particular input $\mathbb{N}(Y_{\text{on}})$ as equal to 1 if the outcome $[\hat{s}_1^C \hat{s}_2^C]$ is equal to $[\hat{s}_1 \hat{s}_2]$, and 0 if it is incorrect. For the ODE solver, this is denoted as

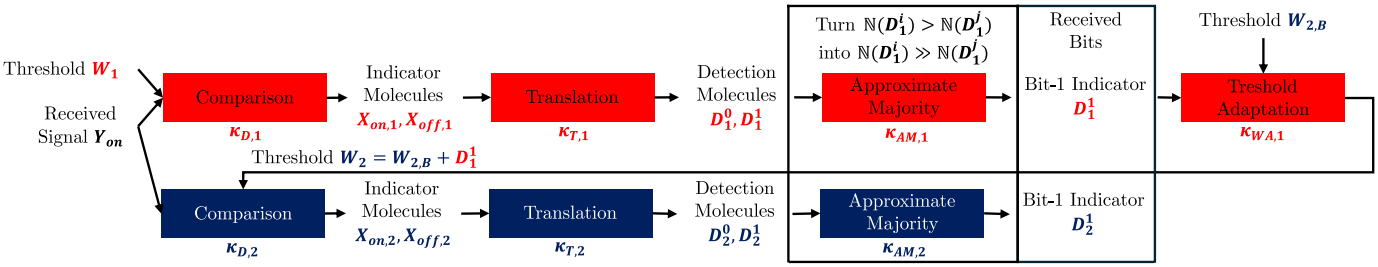

Fig. 4. Proposed ChemSICal structure: A CRN implementing a two-stage SIC algorithm on the RX side. Input: Y_{on}; Outputs: D_i^0, D_i^1, $i \in \{1, 2\}$

TABLE I
COMMUNICATION SYSTEM PARAMETERS

Parameter	Symbol	Values
TX distances	$\{d_1, d_2\}$	$\{10, 12\}$ µm
RX radius	r	1 µm
Diffusion coefficient	D	10^{-9} $\frac{\text{m}^2}{\text{s}}$
Molecules per pulse	N_{TX}	10^6 molecules
Detection thresholds	$\{\tau_1, \tau_2^0, \tau_2^1\}$	{231, 78, 386} molecules

TABLE II
CRN INITIAL VALUES AND PARAMETERS

Parameter	Symbol	Initial Value (Baseline)
Input Species	Y_{on}	$0 \leq \mathbb{N}(Y_{\text{on}}) < 600$
Result Species	$X_{on,1}$	{154, 155, 156, 157}
	$X_{off,1}$	{154, 155, 156, 157}
	$X_{on,2}$	83
	$X_{off,2}$	84
Detection Species	$\{D_1^0, D_1^1, D_2^0, D_2^1\}$	{0,0,0,0}
Threshold Species	W_1	231
	W_2	{75, 76, 77, 78}
	$W_{2,B}$	{75, 76, 77, 78}
Helper Species	$\{B_1, B_2\}$	{0,0}
RRCs	$\kappa_{\text{AM},2}$	{0.8, 1, 1.2, 1.4, 1.6, 3}·10^{-3}
	Other κ_i	See set 5 in Table III

$c[\mathbb{N}(Y_{\text{on}})] \in \{0, 1\}$, or for a single trajectory j generated by the SSA solver, as $c_j[\mathbb{N}(Y_{\text{on}})] \in \{0, 1\}$.

2) *Probability of Correct Detection*: This corresponds to the percentage of trajectories that result in a correct result, given a particular input $\mathbb{N}(Y_{\text{on}})$. It is denoted and calculated as $P_{\text{d}}[\mathbb{N}(Y_{\text{on}})] = \frac{1}{N_{\text{traj}}} \sum_{j=1}^{N_{\text{traj}}} c_j[\mathbb{N}(Y_{\text{on}})]$.
3) *Input-Weighted Probability of Error*: The errors must be weighted according to the PMF given in Eq. (2), such that errors for unlikely inputs are less influential compared to errors for inputs that occur often. We denote the input PMF as $p_{n_{\text{s}}}[\mathbb{N}(Y_{\text{on}})]$. The weighted error probability can be calculated as $P_{\text{e}} = \sum_{\mathbb{N}(Y_{\text{on}})} p_{\text{n}_{\text{s}}}[\mathbb{N}(Y_{\text{on}})] \cdot P_{\text{d}}[\mathbb{N}(Y_{\text{on}})]$.

IV. EVALUATION AND OPTIMIZATION

In the following, we will take a closer look at the performance of the ChemSICal model using the ODE and SSA solver. Recall that a non-chemical version of DBMC-NOMA and a simple DBMC network was described in Section II. For the following evaluation, the parameters in Table I define the communication scenario. The detection thresholds are assumed to be chosen optimally using exhaustive search for the given scenario [5]. Other options such as heuristic optimization using pilot symbols [12] have also been proposed. Using results from [5], the bit error probability (BEP) of the non-chemical network is approximately $P_{\text{e,ideal}} \approx 10^{-6}$. Additionally, the corresponding chemical parameters, initial concentrations and RRCs, are listed in Table II. Unless otherwise stated, the parameters marked as *baseline* will be used. These correspond to the parameters that are translated from the optimal non-chemical parameters according to the relationships for detection thresholds derived in Section III-A.

A. Reaction Rate Constants

The first crucial evaluation step is the choice of RRCs for each reaction block. As the design space here is very large and the resources needed for systematic optimization are quite extensive, in this work we focus on a first preliminary choice

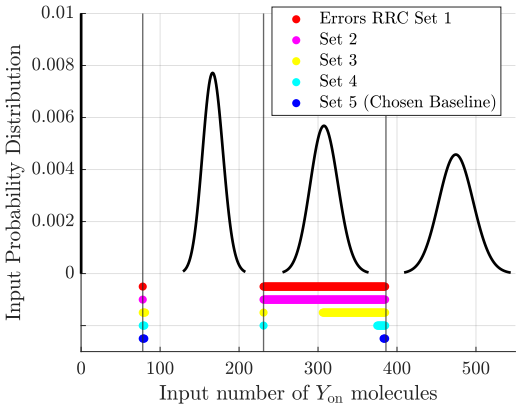

Fig. 5. Comparison of error distributions obtained from the ODE solver for different RRC sets (see Table III). *Set 5* is chosen as baseline for further evaluation. The input probability distribution (see Eq. (2) is also shown.

of the RRCs based on iteratively improving the number of correct detections $c[\mathbb{N}(Y_{\text{on}})]$ using the ODE solver. Figure 5 depicts the observed errors over the different input values for five different sets of RRCs. The associated values can be seen in Table III.

In all our evaluations, we use a normalized time axis as well as normalized RRCs relative to 1, as all RRCs could be multiplied by the same scalar value and all the results would simply be scaled on the time axis. The starting point, *set 1*, is setting all RRCs $\kappa_i = 1$. Here, we see a significant number of errors over a large section of the input space including very likely values, where $[\hat{s}_1 \hat{s}_2] = [10]$. This is largely due to the fact that the reactions for TX_2 will start computing the binary decision before the threshold adaptation reaction has correctly increased $\mathbb{N}(W_2)$. The input is compared to the wrong threshold and the CRN returns $\hat{s}_2^C = 1$ incorrectly. Once the approximate majority block has reached a steady-

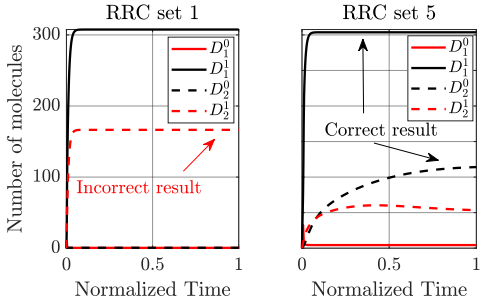

Fig. 6. Comparison of two different sets of RRCs from Table III with respect to the detection species trajectories. The input is $\mathbb{N}(Y_{\text{on}}) = 300$ and the desired result is for D_1^1 and D_2^0 (in black) to be in the majority.

TABLE III
REACTION CONSTANT SETS UTILIZED IN FIGURE 5.

Set	$\kappa_{D,1}$	$\kappa_{T,1}$	$\kappa_{AM,1}$	$\kappa_{WA,1}$	$\kappa_{D,2}$	$\kappa_{T,2}$	$\kappa_{AM,2}$	ODE Errors
1	1.0	1.0	1.0	1.0	1.0	1.0	1.0	0.25
2	1.0	1.0	1.0	1.0	0.1	0.1	0.1	0.25
3	1.0	1.0	0.1	1.0	0.1	0.1	0.01	0.1382
4	1.0	1.0	0.1	1.0	0.1	0.01	0.001	$3.03 \cdot 10^{-3}$
5	1.0	1.0	0.1	1.0	0.1	0.1	0.001	$3.98 \cdot 10^{-4}$

state it is very hard to reverse it. For higher values of $\mathbb{N}(Y_{\text{on}})$ the errors seemingly disappear, but the underlying issue still remains. The result $\hat{s}_2^C = 1$ is now merely accidentally correct, while the input is still being compared to the wrong value of $\mathbb{N}(W_2)$. Generally, the goal is compute the values within the CRN in the correct order, making reactions happen slower that work with results from previous reaction blocks as inputs. Looking at *sets 2* and *3*, we can see that the issue is not solved by simply slowing down all the reactions for TX_2 (*set 2*), and neither by slowing down the approximate majority blocks by an order of magnitude (*set 3*), although the results for *set 3* suggest that we are moving in the correct direction, with some errors disappearing. Lastly, *set 4* and *5* suggest that the approximate majority reaction for TX_2 should be slowed down even further, while the other reactions associated with TX_2 remain at an only slightly slower speed. A direct comparison of the detection species' trajectories calculated by the ODE solver between *set 1* and *set 5* is shown in Figure 6 for $\mathbb{N}(Y_{\text{on}}) = 300$. The results for *set 1* on the left show that D_2^1 incorrectly dominates because the second comparison and approximate majority block reacts too quickly to the non-adapted incorrect threshold. *Set 5* on the right side corrects the initial rise of D_2^1 and yields the correct result. As a consequence, we will use *set 5* as the baseline choice of RRCs going forward.

B. Stochastic Simulation Algorithm

In this section, the SSA solver will be utilized to obtain more nuanced results about the ChemSICal model. For every configuration of parameters, $N_{\text{traj}} = 500$ trajectories per input concentration were generated to calculate estimates of the metrics described in Section III-B. Figure 7 depicts a plot of the input PMF and $P_d[\mathbb{N}(Y_{\text{on}})]$ for the baseline parameter choices, see Table II, in red. We can observe that P_{d} varies between 0.5 and 1, with dips towards 0.5 corresponding to the position of the detection thresholds, thereby forming an inverse shape with respect to the input PMF. This is the

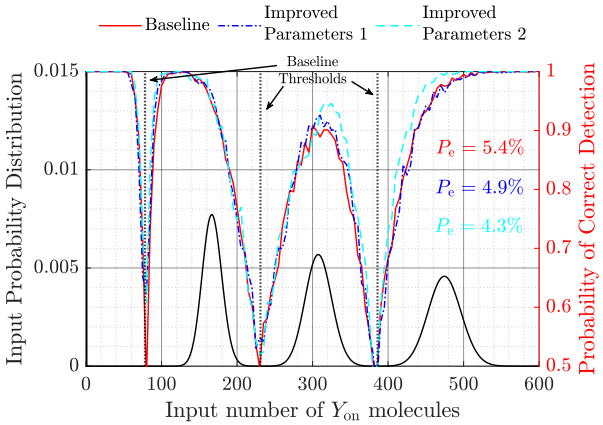

Fig. 7. Plot showing the input PMF and the probability of correct detection P_d over the input values $\mathbb{N}(Y_{\text{on}})$ for $N_{\text{traj}} = 500$ using the SSA solver. For *Improved Parameters 1*, the chemical species for the detection thresholds have been adjusted to $\{\tau 2^0, \tau_2^1\} = \{76, 388\}$. For *Improved Parameters 2*, the thresholds as well as the RRC $\kappa_{\text{AM},2}$ have been adjusted to $\{\tau 2^0, \tau_2^1, \kappa_{\text{AM},2}\} = \{76, 388, 0.0016\}$. The adjustments are based on the sensitivity analysis shown in Figure 8.

desired behavior, as errors occur primarily for unlikely input values, resulting in an input-weighted error probability of $P_{\text{e}} = 0.054$ for the baseline ChemSICal configuration. This implies that the algorithm generally performs successfully in its chemical form. However, we immediately see that $P_{\text{e}} \gg P_{\text{e,ideal}}$, i.e., the ChemSICal model adds significantly more errors to the system compared to the inherent BEP. As a consequence, any optimization of the error probability of the ChemSICal model is several orders of magnitude more impactful, even at the expense of increasing the non-chemical inherent error probability $P_{\text{e,ideal}}$. Therefore, we will look into this in the following.

C. Parameter Adaptation

Looking at the baseline P_{d} plot in Figure 7, the most error-prone regions of the input-space are situated around the thresholds, indicating some potential for optimization there. The figure also shows the values of the targeted baseline thresholds, as presented in Table I. While the minima of P_{d} largely align with the thresholds, they do not match exactly. In fact, a closer look at Figure 7 and an investigation of the trajectories around the thresholds reveals that the *de facto* thresholds, i.e., the values at which the ChemSICal model exhibits a switch in behavior, are slightly higher than desired for τ_2^0, and slightly lower for τ_2^1. Therefore, we conduct a preliminary analysis of the impacts of changing the thresholds from the suggested optimal values. Figure 8 depicts the resulting values of P_{e} for a decrease in τ_2^0 and simultaneous increase in τ_2^1, corresponding to changes in $\mathbb{N}(W_{2,\text{B}})$ and $\mathbb{N}(X_{\text{on},i}), \mathbb{N}(X_{\text{off},i})$. We observe a local optimum configuration with $\{\tau_2^0, \tau_2^1\} = \{76, 388\}$, for which the error probability improves by almost 10% to 0.049. Figure 7 depicts the resulting $P_d[\mathbb{N}(Y_{\text{on}})]$ (denoted as *Improved Parameters 1*), where a visible increase of the detection probability around τ_1^0 and in the error-prone region $300 < \mathbb{N}(Y_{\text{on}}) < 400$ can be observed.

Additionally, we have seen in Section IV-A that the approx-

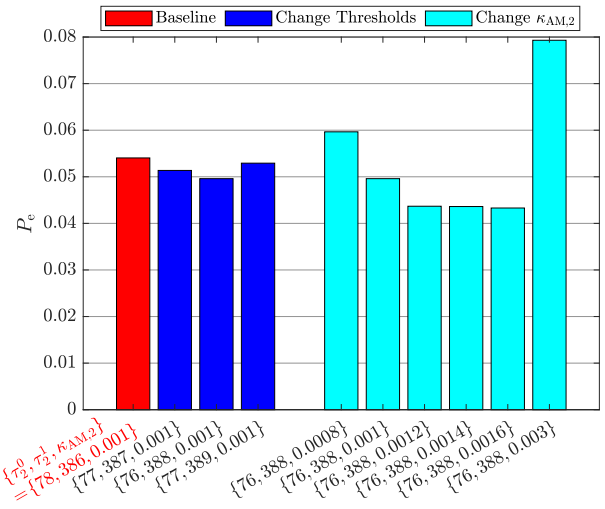

Fig. 8. Sensitivity analysis of thresholds τ_1^0 and τ_1^1, and RRC $\kappa_{\mathrm{AM},2}$, which controls the binary decision for TX_2. The y-axis depicts the input-weighted error probability P_e for 500 trajectories of the SSA solver.

imate majority reaction block for TX_2, and in particular its RRC $\kappa_{\mathrm{AM},2}$, is decisive for the performance of the ChemSICal model. Consequently, we will also take a look at a more granular sensitivity analysis around the baseline value. In the following, we will carry over the improved values for the detection thresholds from the prior analysis. Figure 8 shows the resulting P_e for different values of $\kappa_{\mathrm{AM},2}$ in cyan color. We can see that the error probability can be reduced further significantly, by about 10% to 0.043, if the reaction speed is increased up to $\kappa_{\mathrm{AM},2} = 0.0016$. Reducing or further increasing $\kappa_{\mathrm{AM},2}$ will drastically worsen the performance of the ChemSICal model, once again underlining the strong effect of even relatively small changes in RRCs on the performance. Figure 7 also depicts the corresponding $P_\mathrm{d}[\mathbb{N}(Y_\mathrm{on})]$ (denoted as *Improved Parameters 2*). Here, we once again see the largest positive effect in the error-prone range $300 < \mathbb{N}(Y_\mathrm{on}) < 400$. The increased RRC leads to a narrower dip in P_d. This only works up to a certain point, as we have seen in Section IV-A, since the approximate majority reaction has to be slow enough for the previous reactions to always deliver the correct results in time.

V. Conclusion

This work has presented ChemSICal, a detailed CRN model capable of executing the SIC algorithm for MA within a DBMC networking scenario. The CRN structure is based on multiple smaller reaction blocks and can run fully simultaneously to extract the transmitted bits from 2 TXs at the RX. Subsequently, both deterministic ODE methods and a SSA were used to investigate the performance of ChemSICal, revealing the behavior of the system under various input conditions. The RRCs were identified as crucial parameters to ensure to correct execution of the algorithm and comparing several iteratively adapted values, a reasonable set of RRCs was found. As the error probability introduced by ChemSICal is found to be much larger than the underlying analytical one, the potential for optimizing the chemical system even at the cost of worsening the significantly smaller inherent BEP was underlined. A preliminary sensitivity analysis of detection thresholds and RRCs showed that the chemical implementation of an algorithm does not necessarily work optimally using the analytical optima found for the non-chemical implementation, but that we need to reevaluate our choices with the chemical behavior of the system in mind, leading to a co-optimization approach between the analytical and the chemical model.

Further work must focus on generalizing and scaling the presented concepts. Approaches such as timing mechanisms and chemical clocks [7] could enable faster and more controlled execution of the CRN. This could open up opportunities for connecting multiple CRNs, such that, for example, the parameter optimization of the thresholds could also be implemented chemically. Additionally, the repeated execution and, therefore, the reset of CRNs must also be taken into account going forward.

References

[1] I. F. Akyildiz, M. Pierobon, S. Balasubramaniam, and Y. Koucheryavy, "The Internet of Bio-Nano Things," *IEEE Commun. Mag.*, Mar. 2015.

[2] P. Hofmann, S. Schmidt, A. Wietfeld, P. Zhou, J. Fuchtmann, F. H. P. Fitzek, and W. Kellerer, "A Molecular Communication Perspective on Detecting Arterial Plaque Formation," *IEEE Trans. Mol. Biol. Multi-Scale Commun.*, vol. 10, p. 458–463, Sept. 2024.

[3] E. Shitiri and H.-S. Cho, "A TDMA-Based Data Gathering Protocol for Molecular Communication via Diffusion-Based Nano-Sensor Networks," *IEEE Sensors Journal*, vol. 21, Sept. 2021.

[4] X. Chen, M. Wen, C.-B. Chae, L.-L. Yang, F. Ji, and K. K. Igorevich, "Resource Allocation for Multiuser Molecular Communication Systems Oriented to the Internet of Medical Things," *IEEE Internet of Things Journal*, vol. 8, Nov. 2021.

[5] A. Wietfeld, S. Schmidt, and W. Kellerer, "DBMC-NOMA: Evaluating NOMA for Diffusion-Based Molecular Communication Networks," in *Proc. IEEE Int. Conf. Commun. (ICC)*, June 2024.

[6] M. Vasić, D. Soloveichik, and S. Khurshid, "CRN++: Molecular programming language," *Natural Computing*, June 2020.

[7] B. Heinlein, L. Brand, M. Egan, M. Schäfer, R. Schober, and S. Lotter, "Closing the Implementation Gap in MC: Fully Chemical Synchronization and Detection for Cellular Receivers," *IEEE Trans. Mol. Biol. Multi-Scale Commun.*, 2024.

[8] S. Angerbauer, W. Haselmayr, F. Enzenhofer, T. Pankratz, R. Khanzadeh, and A. Springer, "Molecular Nano Neural Networks (M3N): In-Body Intelligence for the IoBNT," in *Proc. IEEE Int. Conf. Commun. (ICC)*, June 2024.

[9] A. Wietfeld, S. Schmidt, M. Wendrich, and W. Kellerer, "A Chemical Reaction Network for Successive Interference Cancellation in Molecular Communication Networks," in *Proc. ACM NANOCOM (short work-in-progress paper)*, Oct. 2024.

[10] V. Jamali, A. Ahmadzadeh, W. Wicke, A. Noel, and R. Schober, "Channel Modeling for Diffusive Molecular Communication—A Tutorial Review," *Proc. IEEE*, July 2019.

[11] J. Torres Gómez, K. Pitke, L. Stratmann, and F. Dressler, "Age of information in molecular communication channels," *Digital Signal Processing*, May 2022.

[12] A. Wietfeld, S. Schmidt, and W. Kellerer, "Error Probability Optimization for Non-Orthogonal Multiple Access in DBMC Networks," *IEEE Trans. Mol. Biol. Multi-Scale Commun.*, June 2024.

[13] A. Wietfeld, S. Schmidt, and W. Kellerer, "Non-Orthogonal Multiple Access for Diffusion-Based Molecular Communication Networks," in *Proc. ACM NANOCOM*, Sept. 2023.

[14] J. H. Abel, B. Drawert, A. Hellander, and L. R. Petzold, "GillesPy: A Python Package for Stochastic Model Building and Simulation," *IEEE Life Sciences Letters*, vol. 2, Sept. 2016.

[15] D. T. Gillespie, "Exact stochastic simulation of coupled chemical reactions," *The Journal of Physical Chemistry*, Dec. 1977.